Theoretical Study on the Deglycosylation Mechanism of Rice BGlu1 β-Glucosidase

Jinhu Wang,[a] Qianqian Hou,[a] Xiang Sheng,[a] Jun Gao,[a] Yongjun Liu,*[a,b] and Chengbu Liu[a]

It is proposed that the catalysis of GH1 enzymes follows a double-displacement mechanism involving a glycosylation and a deglycosylation steps. In this article, the deglycosylation step was studied using quantum mechanical/molecular mechanical (QM/MM) approach. The calculation results reveal that the nucleophilic water (Wat1) attacks to the anomeric C_1, and the deglycosylation step experiences a barrier of 21.4 kcal/mol from the glycosyl-enzyme intermediate to the hydrolysis product, in which an oxocarbenium cation-like transition state (TS) is formed. At the TS, the covalent glycosyl-enzyme bond is almost broken (distance of 2.45 Å), and the new covalent bond between the attacking oxygen of the water molecule and C_1 is basically established (length of 2.14 Å). In addition, a short hydrogen bridge is observed between the nucleophilic E386 and the C_2—OH of sugar ring (distance of 1.94 Å) at the TS, which facilitates the ring changing from a chair form to half-chair form, and stabilizes the oxocarbenium cation-like TS.

DOI: 10.1002/qua.24131

Introduction

β-Glucosidases (3.2.1.21) are able to catalyze the hydrolysis of β-glycosidic bonds between the nonreducing end of β-glucan-derived oligosaccharides and glycosides. Based on the amino acid-sequence classified by Henrissat,[1] β-glucosidases belong to the glycoside hydrolase (GH) families GH1, GH3, GH5, GH9, GH30, and GH116.[2,3] Among all these GH families, GH1 is reported mostly due in part to the large number of GH1 isoenzymes with different specificities found in plants.[4] GH1 β-glucosidases have been implicated in a diversity of roles in plants, such as response to biotic and abiotic stresses, defense against herbivores, activation of phytohormones,[5] aromatic volatiles,[6] lignification, and cell wall remodeling.

So far, people have crystallized the structures of GH1 β-glucosidases for bacterial,[7] fungal,[8] and plants (rice, maize, sorghum, and wheat) enzymes.[1,9–19] Among all the plants enzymes, the most well-studied one is rice BGlu1 (namely Os3BGlu7) enzyme, which is identified as a highly expressed iso-enzyme in rice organs with high level of activities, such as flower, seedling shoot and so on.[9,10,20,21] As the most homologous enzyme with that of plants, the rice BGlu1 is more efficiently to hydrolyze cello-oligosaccharides.[22]

The GH1 enzymes, including rice BGlu1, act via a retaining double-displacement mechanism[23] involving a glycosylation and a deglycosylation steps, as shown in Figure 1. The catalytic groups are two glutamate residues. One residue serves as a nucleophile and the other as a general acid/base catalyst, in which a covalent glycosyl-enzyme intermediate is formed with the reaction proceeding. In the glycosylation step, the glycosidic oxygen is first protonated by the acid/base residue. Then, the nucleophilic residue attacks the anomeric carbon to form a α-linked covalent glycosyl-enzyme intermediate. In the deglycosylation step, the intermediate is hydrolyzed by a water molecule, which is activated by the extraction of a proton by the catalytic acid/base residue. The final products are the free sugar and the free enzyme with the protonated acid/base residue. Both in the glycosylation and the deglycosylation steps, the sugar ring acquires transition from a chair conformation ($^4C_1$ ring) at the beginning of the reaction to a half-chair conformation at the transition state (TS, as shown in Fig. 1), back to the $^4C_1$ ring at the product.

The glycosylation[24] and deglycosylation[25] processes for β-glucosidases have been studied via quantum mechanics using DFT methods. In these studies, only simplified models were adopted to mimic the enzymatic reaction. For example, in the study of deglycosylation, the two catalytic residues were simplified with two propanoic acids, and the substrate was modeled by a galactose molecule covalently bound to the nucleophilic residue, and one water molecule was set in an ideal position to attack the anomeric carbon. The calculated barriers ranged from 23.1 to 30.8 kcal/mol depending on the calculation methods and models. Recently, the glycosylation and deglycosylation steps of the endoglucanase (Cellulase Cel5A) were studied using semiempirical quantum mechanical/molecular mechanical (QM/MM) method.[26]

We have studied the glycosylation process in GH1-catalyzed hydrolysis of a β-glycoside using QM/MM method.[27] In this

[a] J. Wang, Q. Hou, X. Sheng, J. Gao, Y. Liu, C. Liu
Key Lab of Colloid and Interface Chemistry, Ministry of Education, School of Chemistry and Chemical Engineering, Shandong University, Jinan, Shandong 250100, China
[b] Y. Liu
Northwest Institute of Plateau Biology, Chinese Academy of Sciences, Xining, Qinghai 810001, China
E-mail: yongjunliu_1@sdu.edu.cn

Contract grant sponsor: Natural Science Foundation of China; contract grant number: 21173129.

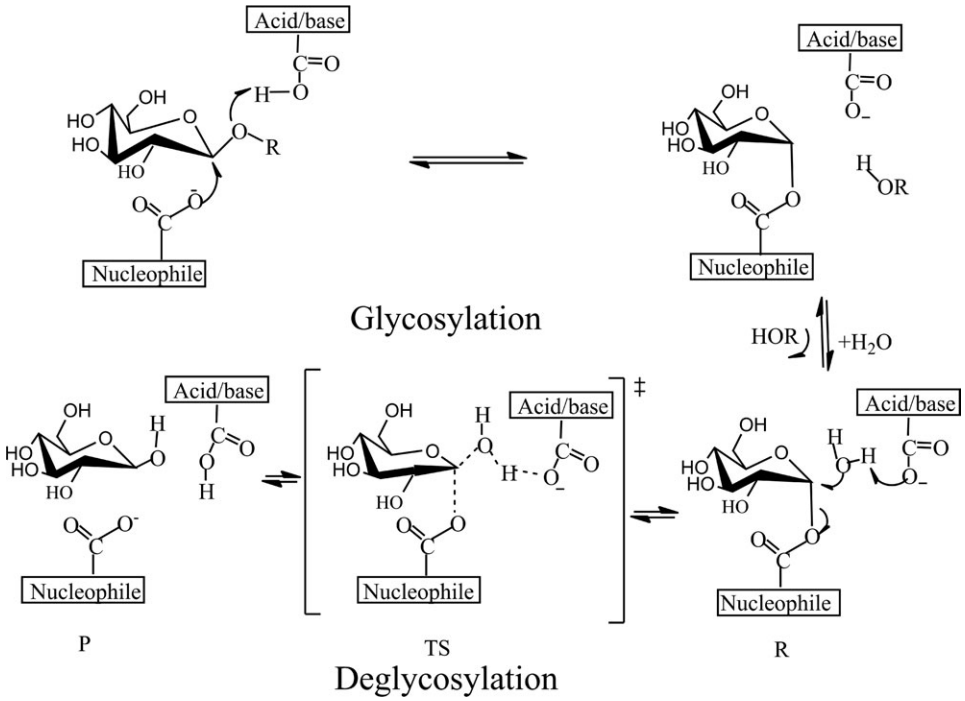

Figure 1. Proposed double displacement mechanism for the β-glucosidases.[23]

article, the deglycosylation step was further studied by using the same approach. In the calculations, the residues that take part in the reaction directly was chosen as QM region and the remaining part of protein and solvent was selected as MM region,[28–31] which were described by quantum mechanics and molecular mechanics, respectively. The combined QM/MM method was used to investigate the catalytic mechanism by rice BGlu1, hoping to achieve a better description of deglycosylation process.

Computational Details

Computational model

The crystallographic data of the enzyme (rice BGlu1 E176Q mutant complexed with laminaribiose, pdb code: 3F5L)[22] was taken from Protein Data Bank. In the modeling, the E176Q mutation was first mutated back to glutamate to obtain a functional active site. The initial structure in this study was the covalent glycosyl-enzyme intermediate obtained by our previous work in the glycosylation step,[27] in which a glucose ring covalently bound to the nucleophilic residue E386 (Fig. 2). All the glutamate residues including E176 were charged in the following molecular dynamics (MD) simulations. Besides, according to the experimental condition, the protonation states of other residues were checked carefully using the VMD program,[32] and the missing hydrogen atoms were added with the help of the HBUILD facility in the CHARMM package.[33] Furthermore, a number of water molecules (5243) were added to solvate the system forming a water sphere of 39 Å radius centered on E176 residue. In the end, the system was neutralized by 9 Cl^- ions at random positions. A neutral system of 23,219 atoms was finally obtained. The prepared system was performed with a series of minimizations and a 1000 ps MD simulation under the CHARMM2227 force field.[34] The obtained structure was further optimized by QM/MM method.

QM/MM calculations

In our model, the QM subsystem contains 55 atoms in the reactant center (which is shown in Fig. 3), including catalytic residues E176 and E386, glucose ring that covalently bounds to residue E386, and a crystal water molecule Wat1. The remaining part of the enzyme and water molecules was defined as the MM region. During the subsequent QM/MM calculations, the QM part was

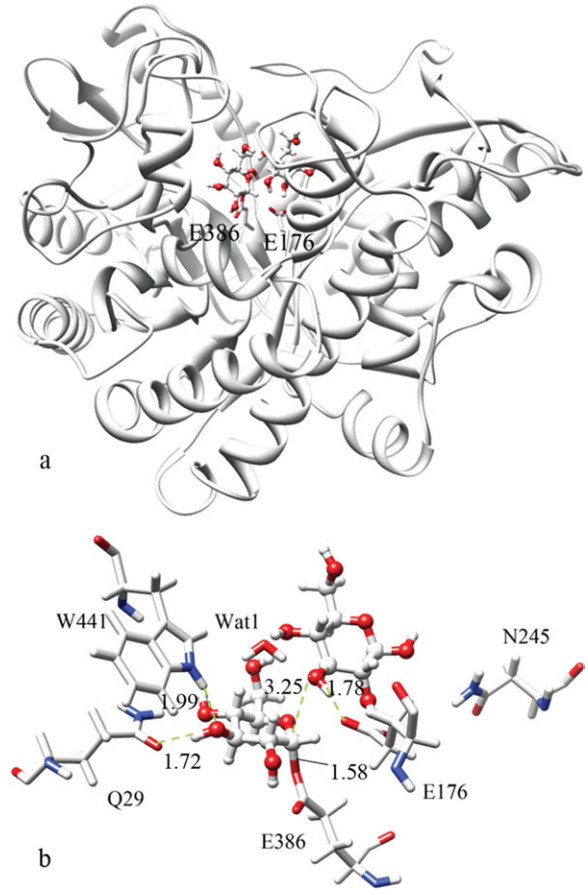

Figure 2. (a) The structure of covalent glycosyl-enzyme intermediate; (b) the corresponding crucial residues in the active site. [Color figure can be viewed in the online issue, which is available at wileyonlinelibrary.com.]

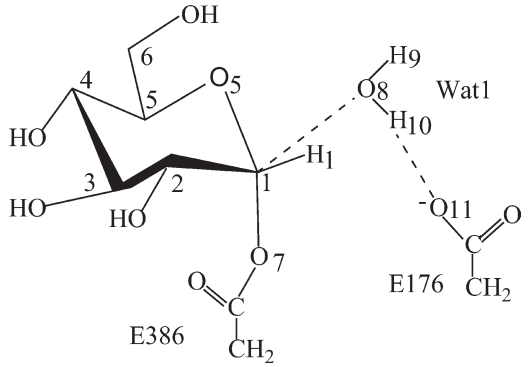

Figure 3. The selected quantum mechanics region in QM/MM calculations.

calculated by quantum mechanics using the B3LYP/6-31G(d,p) by Turbomole module,[35] while the MM region was treated with molecular mechanics under the CHARMM2227 force field by DL-POLY program.[36] During the calculations, the displacement and SCF convergence criterions were set as 1.0×10^{-7} and 4.5×10^{-4} a.u., respectively. The calculations of frequency were performed at the same level, in which no imaginary frequency mode was found for reactant and product, and only one imaginary frequency mode was obtained for the TS. Using the electronic embedding scheme,[37] one-electron Hamiltonian calculations were performed with the MM charges,[38] for the purpose of avoiding hyperpolarization of the QM wave function. The QM/MM boundary was adopted with charge shift model linked by Hydrogen atoms in the QM/MM treatment.[39] The ChemShell package[40] integrating Turbomole and DL-POLY programs was used to perform the QM/MM calculations.

Results and Discussion

The initial structure was the covalent glycosyl-enzyme intermediate obtained by our previous calculation,[27] which is the product of the glycosylation step, as shown in Figure 2. The length of glycosidic bond is 3.25 Å, indicating this bond has been cleaved. Meanwhile, the carboxylate oxygen of nucleophilic residue E386 has already formed a covalent bond with the anomeric carbon (C_1) with length of 1.58 Å. In the following calculations, the leaving group (a glucose ring) has been removed from the system.

The energy paths for deglycosylation step associated with the reaction shown in Figure 4, were calculated using B3LYP/6-31G(d)//CHARMM22 geometrical optimization in an adiabatic mapping procedure.[41] In this work, we scanned the reaction path along the reaction coordinates: $d = r_2 - r_1$, $r_1 = C_1 - O_8$, and $r_2 = O_8 - H_{10}$. The obtained structures of the reactant, TS, and product were reoptimized at the same level and the final structures are shown in Figure 5, and collective variables defining the extent of reaction are shown in Table 1. Frequency calculations gave the unique imaginary frequency of 134.3*i* for the TS, and no imaginary frequency model in reactant and product.

In reactant (Fig. 5a), the distance between the incoming water Wat1 and anomeric carbon C_1 is 3.75 Å. The water Wat1 establishes a hydrogen bond (distance of 1.83 Å) with the carboxylate group of catalytic acid/base E176. Meanwhile, the glucose ring forms the covalent glycosyl-enzyme bond with nucleophilic residue E386 with a length of 1.53 Å. By comparing the same bond in Figures 5a and 2, we can see that this bond has been strengthened as the leaving group departs. In TS (Fig. 5b), the water molecule Wat1 comes close to the anomeric C_1, with its oxygen atom attached to the anomeric center (distance shortens to 2.14 Å from 3.75 Å). At the same time, one proton of Wat1 is getting closer to the carboxylate group of E176, displaying a bond length of 1.55 Å. The distance change of the bond (from 1.83 to 1.55 Å) reveals that it has been strengthened at the TS. Besides, the O—H bond of the Wat1 has extended to 1.03 Å (1.00 Å in Fig. 5a). The little change of the O—H bond in Wat1 indicates the proton transfer to E176 has not yet occurred at this state. At the same stage, the covalent glycosyl-enzyme bond between anomeric C_1 and nucleophile lengthens to 2.45 Å, implying this bond has been broken.

For product (Fig. 5c), the OH group of Wat1 has attached to the anomeric C_1 as the distance between them shortens to1.48 Å. At the same time, the acid/base residue E176 has attracted a proton from Wat1, establishing a new covalent bond (bond length is 1.01 Å). The distance between the carboxyl group of the nucleophilic E386 and C_1 has extended to 2.95 Å, indicating the cleavage of this valence bond is completed.

In the TS, a short hydrogen bridge is established between the nucleophilic residue E386 and the C_2—OH (labeled in Fig. 3) of the sugar ring with a distance of 1.94 Å, where this distance is 2.66 Å for the reactant (Fig. 5a) and 2.65 Å for the product (Fig. 5c). The role of this hydrogen interaction is responsible for lowering the energy barrier (5 kcal/mol) of the TS and the stabilization of this state in the deglycosylation step.[25]

The superposition of reactant, TS, and product is shown in Figure 5d. A structural rearrangement of the sugar ring is observed at the TS. The saccharide ring that attaches the nucleophile planarizes toward the half-chair conformation from the typical chair conformation, which can be seen from the analysis of the changes of dihedral angle C_1—C_2—C_3—O_5 and C_1—C_2—O_5—H_1 (labels given in Fig. 3). The angle of

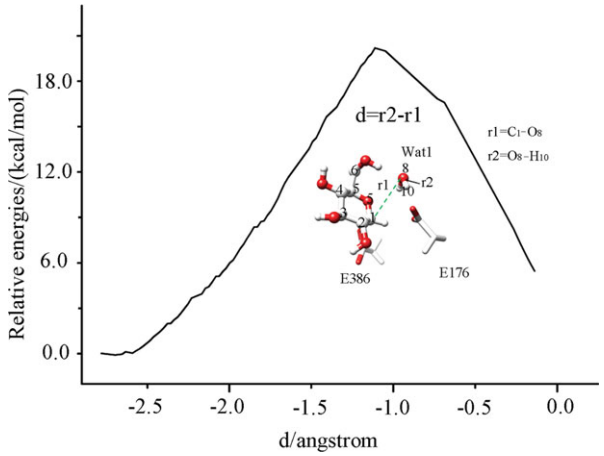

Figure 4. Energy paths for deglycosylation step using the B3LYP/6-31G(d)//CHARMM22 method. The distance (labeled as variable d) in the abscissa shows the difference between variables r2 and r1, while the energy is the total energy when variable d changes. [Color figure can be viewed in the online issue, which is available at wileyonlinelibrary.com.]

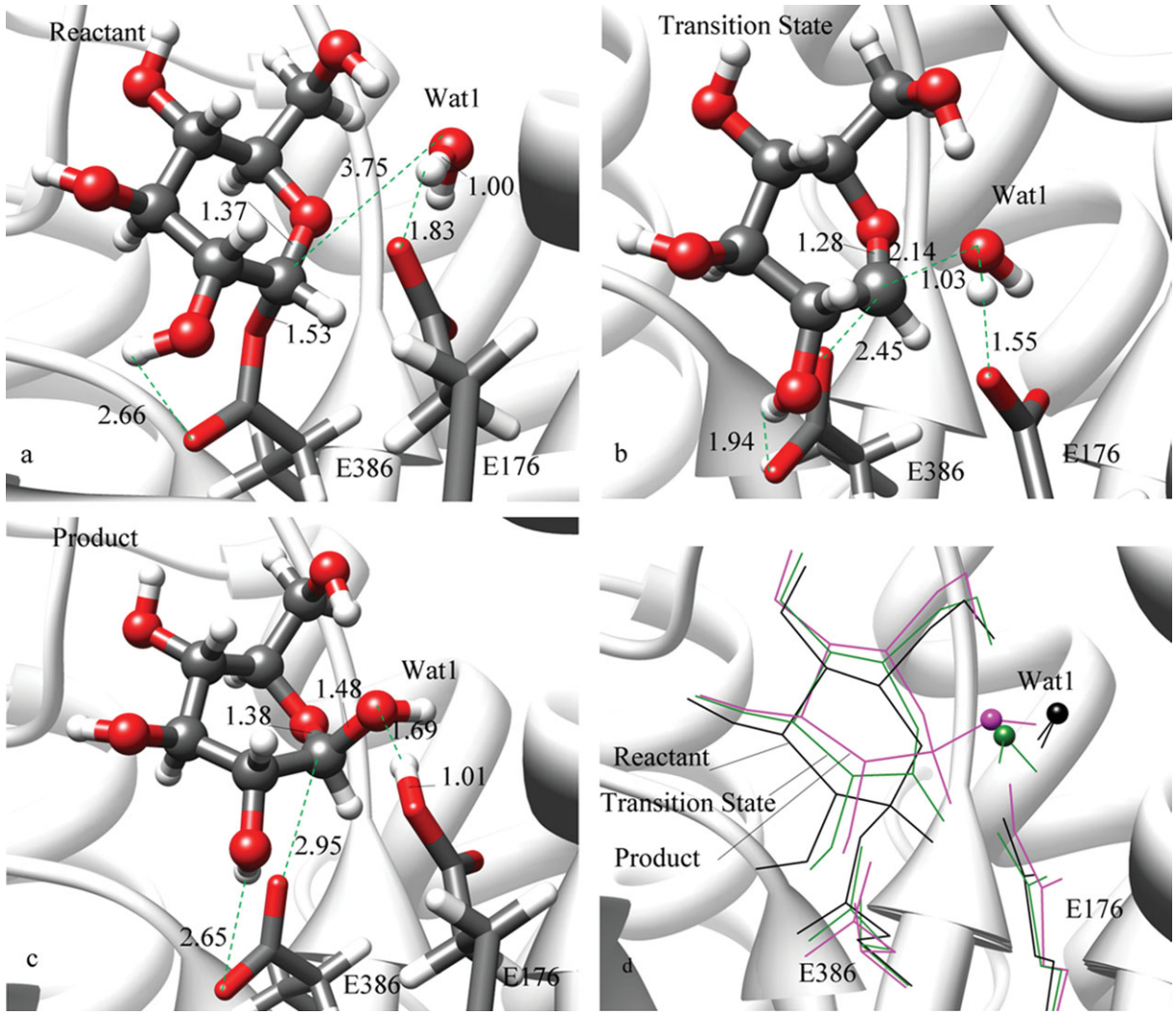

Figure 5. Optimized geometries of reactant (a), TS (b) and product (c). The superposition of three states is also shown for comparison (d). [Color figure can be viewed in the online issue, which is available at wileyonlinelibrary.com.]

C_1—C_2—C_3—O_5 is -24.1° in reactant, and changes to -4.6° in TS and 3.3° in product, while the angles of C_1—C_2—O_5—H_1 are -31.5°, 9.4°, and 33.1° for reactant, TS, and product, respectively. It is supposed that the conformational change from the typical chair conformation to the half-chair form in TS moves the sugar ring closer to the conformation of the oxocarbenium ion TS, and facilitates the "in-line" attack of the oxygen of nucleophilic water Wat1 to anomeric C_1, which can stabilize the oxocarbenium ion-like TS.[42] Besides, the flattening of the chair conformational of the sugar ring at the TS also results in the electron transfer from O_5 to anomeric C_1, creating a partial double bond character (C_1=O_5) that induces a planar arrangement of the bonds around.[25] For the purpose of understanding the bonding nature between C_1 and O_5, the length of the bond C_1—O_5 was measured along the reaction coordinate. We can see that length of the C_1—O_5 changes from 1.37 Å in reactant (Fig. 5a), to 1.28 Å in TS (Fig. 5b), and 1.38 Å in product (Fig. 5c). The bond length in TS which is just between that of a "pure" C=O double (1.23 Å) and C—O simple (1.44 Å) bonds.[25] All data mentioned above were obtained from the optimized geometries in Figure 5.

After identifying the geometries of reactant, TS, and product, single point calculations were performed using 6-31++G(2d,2p) basis set. The obtained energy barrier of the deglycosylation reaction is only 21.4 kcal/mol, which is smaller than that of the DFT calculations.[25] Brás et al. calculated this barrier using simple models with different functionals, such as BB1K, BHandHLYP, MPW1K, MPWB1K, and B3LYP functionals, and post-Hartree–Fock methods [MP2, MP3, MP4, and QCISD(T)]. All the obtained values were bigger than 23 kcal/mol. Comparing the energies of the reactant and product, one

Table 1. Bond distances (Å) of the optimized structures along the reaction pathway.

	Reactant	TS	Product
C_1—O_5	1.37	1.28	1.38
C_1···O_8	3.75	2.14	1.48
O_8—H_{10}	1.00	1.03	1.69
H_{10}···O_{11}	1.83	1.55	1.01
C_1—O_7	1.53	2.45	2.95

can see that the reaction of the deglycosylation process is endothermic as the relative energy of the product is 3.5 kcal/mol higher than that of reactant.

According to the deglycosylation step, the subsystem of the QM region keeps the same throughout the calculations, so the number of wave functions remains unchanged in the modeling. Furthermore, a bigger basis function is used. Therefore, the basis set superposition error is thought to be small enough to be ignored for simplifying the calculations.

Conclusions

In this work, the deglycosylation step of substrate hydrolysis of wildtype rice BGlu1 β-glucosidase was studied by QM/MM calculations. Our results show that the reactant experiences an oxocarbenium cation-like TS to the product with an energy barrier of 21.4 kcal/mol. The covalent glycosyl-enzyme bond established between the nucleophilic residue E386 and anomeric C_1 is almost broken (about 2.45 Å away), while the new covalent bond between the attacking oxygen of the incoming water molecule Wat1 and C_1 has not been completely established (bond length is approximately 2.14 Å) at TS. The proton of Wat1 gets closer to acid/base E176, but is still far from E176 (length about 1.55 Å). Besides, a short hydrogen bridge is formed between the nucleophilic E386 and the C_2—OH of the sugar ring, which facilitates the conformational change toward the half-chair form at the TS and helps to stabilize the oxocarbenium cation-like TS.

Keywords: QM/MM · deglycosylation · β-glucosidases · laminaribiose · reaction mechanism

How to cite this article: J. Wang, Q. Hou, X. Sheng, J. Gao, Y. Liu, C. Liu, *Int. J. Quantum Chem.* **2013**, *113*, 1071–1075. DOI: 10.1002/qua.24131

[1] B. Henrissat, *Biochem. J.* **1991**, *280,* 309.
[2] B. Henrissat, B. L. Cantarel, P. M. Coutinho, C. Rancurel, T. Bernard, V. Lombard, *Nucleic Acids Res,* **2009**, *37,* 233.
[3] J. R. K. Cairns, A. Esen, *Cel. Mol. Life Sci.* **2010**, *67,* 3389.
[4] J. R. K. Cairns, R. Opassiri, B. Pomthong, T. Onkoksoong, T. Akiyama, A. Esen, *BMC Plant Biol* **2006**, *6,* 33.
[5] B. Brzobohaty, I. Moore, P. Kristoffersen, L. Bako, N. Campos, J. Schell, K. Palme, *Science* **1993**, *262,* 1051.
[6] M. Mizutani, H. Nakanishi, J. Ema, S. J. Ma, E. Noguchi, M. Inohara-Ochiai, M. Fukuchi-Mizutani, M. Nakao, K. Sakata, *Plant Phys.* **2002**, *130,* 2164.
[7] P. Isorna, J. Polaina, L. Latorre-Garcia, F. J. Canada, B. Gonzalez, J. Sanz-Aparicio, *J. Mol. Biol.* **2007**, *371,* 1204.
[8] Y. Nijikken, T. Tsukada, K. Igarashi, M. Samejima, T. Wakagi, H. Shoun, S. Fushinobu, *FEBS Lett.* **2007**, *581,* 1514.
[9] W. Chuenchor, S. Pengthaisong, J. Yuvaniyama, R. Opassiri, J. Svasti, J. R. K. Cairns, *Acta Crystallogr. Sect. F Struct. Biol. Cryst. Commun.* **2006**, *62,* 798.
[10] W. Chuenchor, S. Pengthaisong, R. C. Robinson, J. Yuvaniyama, W. Oonanant, D. R. Bevan, A. Esen, C. J. Chen, R. Opassiri, J. Svasti, J. R. K. Cairns, *J. Mol. Biol.* **2008**, *377,* 1200.
[11] T. Barrett, C. G. Suresh, S. P. Tolley, E. J. Dodson, M. A. Hughes, *Structure* **1995**, *3,* 951.
[12] W. P. Burmeister, S. Cottaz, H. Driguez, S. Palmieri, B. Henrissat, *Structure* **1997**, *5,* 663.
[13] M. Czjzek, M. Cicek, V. Zamboni, D. R. Bevan, B. Henrissat, A. Esen, *Proc. Natl. Acad. Sci. USA* **2000**, *97,* 13555.
[14] M. Czjzek, M. Cicek, V. Zamboni, W. P. Burmeister, D. R. Bevan, B. Henrissat, A. Esen, *Biochem J.* **2001**, *354,* 37.
[15] L. Verdoucq, M. Czjzek, J. Moriniere, D. R. Bevan, A. Esen, *J. Biol. Chem.* **2003**, *278,* 25055.
[16] L. Verdoucq, J. Moriniere, D. R. Bevan, A. Esen, A. Vasella, B. Henrissat, M. Czjzek, *J. Biol. Chem.* **2004**, *279,* 31796.
[17] M. Sue, K. Yamazaki, S. Yajima, T. Nomura, T. Matsukawa, H. Iwamura, T. Miyamoto, *Plant Phys.* **2006**, *141,* 1237.
[18] L. Barleben, S. Panjikar, M. Ruppert, J. Koepke, J. Stockigt, *Plant Cell* **2007**, *19,* 2886.
[19] S. Seshadri, T. Akiyama, R. Opassiri, B. Kuaprasert, J. K. Cairns, *Plant Phys.* **2009**, *151,* 47.
[20] R. Opassiri, J. R. K. Cairns, T. Akiyama, O. Wara-Aswapati, J. Svasti, A. Esen, *Plant Sci.* **2003**, *165,* 627.
[21] R. Opassiri, Y. L. Hua, Wara-O. Aswapati, T. Akiyama, J. Svasti, A. Esen, J. R. K. Cairns, *Biochem. J.* **2004**, *379,* 125.
[22] W. Chuenchor, S. Pengthaisong, R. C. Robinson, J. Yuvaniyama, J. Svasti, J. R. K. Cairns, *J. Struct. Biol.* **2011**, *173,* 169.
[23] D. E. Koshland, S. S. Stein, *J. Biol. Chem.* **1954**, *208,* 139.
[24] N. F. Brás, S. A. Moura-Tamames, P. A. Fernandes, M. J. Ramos, *J. Comput. Chem.* **2008**, *29,* 2565.
[25] N. F. Brás, M. J. Ramos, P. A. Fernandes, *J. Mol. Struct. Theochem.* **2010**, *946,* 125.
[26] D. G. Xu, J. L. Liu, X. M. Wang, *J. Phys. Chem. B* **2010**, *114,* 1462.
[27] J. H. Wang, Q. Q. Hou, L. H. Dong, Y. J. Liu, C. B. Liu, *J. Mol. Graph. Model.* **2011**, *30,* 148.
[28] A. Warshel, M. Levitt, *J. Mol. Biol.* **1976**, *103,* 227.
[29] M. J. Field, P. A. Bash, M. Karplus, *J. Comput. Chem.* **1990**, *11,* 700.
[30] J. L. Gao, D. G. Truhlar, *Annu. Rev. Phys. Chem.* **2002**, *53,* 467.
[31] H. M. Senn, W. Thiel, *Angew. Chem. Int. Ed. Engl.* **2009**, *48,* 1198.
[32] W. Humphrey, A. Dalke, K. Schulten, *J. Mol. Graph.* **1996**, *14,* 33.
[33] B. R. Brooks, R. E. Bruccoleri, B. D. Olafson, D. J. States, S. Swaminathan, M. Karplus, *J. Comput. Chem.* **1983**, *4,* 187.
[34] A. D. MacKerell, Jr., D. Bashford, M. Bellot, R. L. Dunbrack, Jr., J. D. Evanseck, M. J. Field, S. Fischer, J. Gao, H. Guo, S. Ha, D. Joseph-McCarthy, L. Kuchnir, K. Kuczera, F. T. K. Lau, C. Mattos, S. Michnick, T. Ngo, D. T. Nguyen, B. Prodhom, W. E. Reiher, III., B. Roux, M. Schlenkrich, J. C. Smith, R. Stote, J. Straub, M. Watanabe, J. Wi_orkiewicz-Kuczera, D. Yin, M. Karplus, *J. Phys. Chem. B* **1998**, *102,* 3586.
[35] R. Ahlrichs, M. Bar, M. Haser, H. Horn, C. Kolmel, *Chem. Phys. Lett.* **1989**, *162,* 165.
[36] W. Smith, T. R. Forester, *J. Mol. Graph. Model.* **1996**, *14,* 136.
[37] D. Bakowies, W. Thiel, *J. Phys. Chem.* **1996**, *100,* 10580.
[38] P. Sherwood, A. H. de Vries, S. J. Collins, S. P. Greatbanks, N. A. Burton, M. A. Vincent, I. H. Hillier, *Faraday Discuss.* **1997**, *106,* 79.
[39] A. H. de Vries, P. Sherwood, S. J. Collins, A. M. Rigby, M. Rigutto, G. J. Kramer, *J. Phys. Chem. B* **1999**, *103,* 6133.
[40] P. Sherwood, A. H. de Vries, M. F. Guest, G. Schreckenbach, C. R. A. Catlow, S. A. French, A. A. Sokol, S. T. Bromley, W. Thiel, A. J. Turner, S. Billeter, F. Terstegen, S. Thiel, J. Kendrick, S. C. Rogers, J. Casci, M. Watson, F. King, E. Karlsen, M. Sjovoll, A. Fahmi, A. Schafer, C. Lennartz, *J. Mol. Struct. Theochem.* **2003**, *632,* 1.
[41] H. L. Woodcock, M. Hodoscek, B. R. Brooks, *J. Phys. Chem. A* **2007**, *111,* 5720.
[42] D. L. Zechel, S. G. Withers, *Acc. Chem. Res.* **2000**, *33,* 11.

Received: 25 November 2011
Revised: 16 March 2012
Accepted: 19 March 2012
Published online on 13 April 2012